CrossMark

electronic reprint

STRUCTURAL SCIENCE
CRYSTAL ENGINEERING
MATERIALS

ISSN: 2052-5206
journals.iucr.org/b

Charge distribution as a tool to investigate structural details. IV. A new route to heteroligand polyhedra

Massimo Nespolo

Acta Cryst. (2016). B**72**, 51–66

IUCr Journals
CRYSTALLOGRAPHY JOURNALS ONLINE

Copyright © International Union of Crystallography

Author(s) of this paper may load this reprint on their own web site or institutional repository provided that this cover page is retained. Republication of this article or its storage in electronic databases other than as specified above is not permitted without prior permission in writing from the IUCr.

For further information see http://journals.iucr.org/services/authorrights.html

Acta Cryst B
STRUCTURAL SCIENCE
CRYSTAL ENGINEERING
MATERIALS
ISSN 2052-5206

Charge distribution as a tool to investigate structural details. IV. A new route to heteroligand polyhedra

Massimo Nespolo*‡

Department of Geology and Mineralogy, Faculty of Science, Kyoto University, Kitashirakawaoiwake-cho, Sakyo-ku, Kyoto-shi, 606-8502, Japan. *Correspondence e-mail: massimo.nespolo@crm2.uhp-nancy.fr

Received 25 August 2015
Accepted 14 October 2015

Edited by M. Dusek, Academy of Sciences of the Czech Republic, Czech Republic

‡ On leave from: Université de Lorraine, CRM2, UMR 7036, Vandoeuvre-lès-Nancy, F-54506, France, and CNRS, CRM2, UMR 7036, Vandoeuvre-lès-Nancy, F-54506, France.

Dedicated to the memory of Professor Rudolf Hoppe

Keywords: charge distribution; effective coordination number; heteroligand polyhedra; bond strength.

A new route to apply the charge distribution (CHARDI) method to structures based on heteroligand coordination polyhedra is presented. The previous algorithm used scale factors computed in an iterative way based on the assumption (which turned out to be not always correct) that a real over–under bonding effect affects mainly the anionic charges of each single anion, without grossly modifying the total charge of each type of anion. The new, more general approach is not based on any *a priori* assumption but treats separately the homoligand sub-polyhedra and attributes to each type of atom a fraction of the charge of the atom coordinated to it, computed in a self-consistent iterative way. The distinction between the bonding and non-bonding contact is also redefined in terms of the mean fictive ionic radii (MEFIR), without the need of an empirical parameter, used in the previous algorithm. CHARDI equations are generalized in terms of the new approach and a series of examples is presented.

1. Introduction

Charge distribution (Hoppe *et al.*, 1989; Nespolo *et al.*, 1999, 2001; Eon & Nespolo, 2015), usually shortened as CHARDI, is the most recent extension of Pauling's (1929) concept of bond strength. It fundamentally differs from approaches based on the *R*–*s* curves like the bond valence (BV) method (Brown, 1978) by adopting a Madelung-type (point-charge) description of crystal structures which does not need the use of empirical parameters frequently redefined and re-refined on which instead the BV method depends (Bosi, 2014*a*,*b*; Gagné & Hawthorne, 2015). To assign a strength to each bond, CHARDI directly exploits the bond distances in each coordination polyhedron: the bond strength, called *bond weight* here, is a function of the ratio of each bond length to the minimal bond length in the same polyhedron. The bond weight is therefore a dimensionless geometric concept which is then used to distribute the formal oxidation number (the 'charge') of each atom to its neighbours. The advantage of the CHARDI approach is precisely the direct use of experimental bond lengths without empirical parameters. On the other hand, the Madelung-type approach in which each atom is described as a point charge makes less straightforward the treatment of heteroligand polyhedra, *i.e.* polyhedra having chemically different atoms, and thus possibly significantly different size, at their corners (Mohri, 2000). We have previously overcome this problem by the introduction of scale factors computed through an iterative procedure that makes them independent from the definition of atomic or ionic radius, and is formally reminiscent of the iterative calculation of bond valences that Brown (1977) adopted to apply his 'equal valence rule'. This gave satisfactory results in the

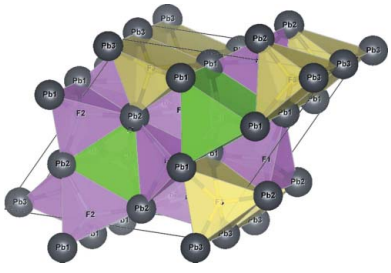

© 2016 International Union of Crystallography

electronic reprint

classical description of crystal structures where electropositive atoms ('cations') are at the centre and electronegative atoms ('anions') at the corner of the polyhedra (Nespolo *et al.*, 2001). The recent generalization of the algorithm to treat structures better described in terms of anion-centred polyhedra (Eon & Nespolo, 2015), called 'reverse' structures by Beck (2014) – as opposite to 'direct' structures based on cation-centred polyhedra – led us to reconsider this problem in an effort to obtain a more general and satisfactory treatment of heteroligand polyhedra bringing atoms of largely different size at their corners. After a short presentation of the method, we show that the dual description as cation-centred and anion-centred proves to be the clue for a satisfactory treatment of these structures.

In the presentation below a relatively large number of symbols is used. To improve the readability of the text, we present a short glossary of symbols and terms used in following text.

1.1. Glossary of symbols and terms

PC(ij): an atom inside a coordination polyhedron, of the ith chemical species and the jth crystallographic type.

V(rs): an atom at the corner (vertex) of a coordination polyhedron, of the rth chemical species and the sth crystallographic type.

$R(i)$, $R(r)$: the ionic radii of PC(ij) and V(rs), respectively (which do not depend on the crystallographic type j or s).

$h(ij)$, $h(rs)$: the multiplicity of the Wyckoff position occupied by PC(ij) and V(rs), respectively.

$q(ij)$, $q(rs)$: the formal oxidation number ('charge') of PC(ij) and V(rs), respectively; these are input values of the CHARDI algorithm.

$Q(ij)$, $Q(rs)$: the charge of PC(ij) and V(rs), respectively, computed as the result of the distribution of $q(ij)$ and $q(rs)$; these are output values of the CHARDI algorithm.

$d(ij \rightarrow rs)_L$: the Lth distance between PC(ij) and V(rs), listed in increasing order.

FIR$(ij \rightarrow rs)_L$: the fictive ionic radius corresponding to $d(ij \rightarrow rs)_L$.

MEFIR$(ij \rightarrow r)$: the mean fictive ionic radius of PC(ij) in the coordination sub-polyhedron having only V atoms of the rth chemical species at its corners.

MEFIR(ij): the mean fictive ionic radius of PC(ij) in the whole coordination polyhedron.

$d(ij \rightarrow r)$: the weighted average distance between PC(ij) and the V atoms of the rth chemical species to which it is coordinated.

$w(ij \rightarrow rs)_L$: the weight of the Lth distance between PC(ij) and V(rs) ('bond strength' in the CHARDI approach).

ECoN$(ij \rightarrow r)$: the effective coordination number of PC(ij) with respect to V atoms of the rth chemical species to which it is coordinated.

ECoN(ij): the effective coordination number of PC(ij) with respect to all the V atoms to which it is coordinated.

ΔECoN$(ij \rightarrow rs)$: the fraction of ECoN$(ij \rightarrow r)$ coming from the V atom of the sth crystallographic type.

$\Delta q(ij \rightarrow rs)$: the fraction of $q(ij)$ received by V(rs).

$\Delta Q(i \rightarrow rs)$: the fraction of charge that each V atom shares with the ith chemical species of PC atom.

$\Delta Q(ij \rightarrow r)$: the fraction of charge that each PC-atom shares with the rth chemical species of V atom.

2. FIR, MEFIR and ECoN

Atoms in a crystal structure are classified in 'polyhedron-centring atoms' (**PC atoms**) and 'vertex (corner) atoms' (**V atoms**) (Eon & Nespolo, 2015). The assignment of cations or anions to each of the two categories can be done interchangeably.

PC atoms and V atoms are indicated as PC(ij) and V(rs), respectively, where i and r identify the atomic site, j and s the crystallographic type. For example, in the structure of potassium selenotrithionate, $K_2SeS_2O_6$, analysed below, the asymmetric unit contains one formula unit, with two crystallographic types of K and S each, one of Se and six of O. By treating cations as PC atoms ij takes the four values 11, 12, 21 and 22 for K1, K2, S1 and S2, and rs takes seven values 11 and 21 to 26 for Se and O1 to O6. If the anions are treated as PC atoms, the corresponding indices ij and rs are simply exchanged.

The formal charges (which become weighted average charges in the case of isomorphic substitutions) are indicated as $q(ij)$ and $q(rs)$ and depend on j or s through the site occupation factor (*sof*): for *sof* = 1, all the PC atoms with the same i, as well as all the V atoms with the same r, have the same q. Similarly, the multiplicity of the Wyckoff position is indicated as $h(ij)$ and $h(rs)$. The Lth bond length between PC(ij) and V(rs) is indicated as $d(ij \rightarrow rs)_L$. For computational purposes, the bond lengths are ordered in increasing length with respect to i, j and r, $d(ij \rightarrow rs)_1$ being the shortest one and s a sort of dummy index at this stage.

Pauling's (1929) statement that in ionic compounds the distance between two bonded ions with charges of opposite sign should be nearly identical to the sum of the ionic radii $R(i)$ and $R(r)$ was generalized by Hoppe (1979) with the introduction of the fictive ionic radii FIR$(ij \rightarrow rs)_L$ concept, defined as

$$\mathrm{FIR}(ij \rightarrow rs)_L = d(ij \rightarrow rs)_L \cdot \frac{R(i)}{R(i) + R(r)}. \qquad (1)$$

In the case of uniform coordination polyhedra,[1] all the FIR$(ij \rightarrow rs)_L$ are identical and the deviation from the ionic radius may be read as a measure of the departure from the pure ionic character of the bond. For non-uniform polyhedra, instead, the concept of ionic radius is less well defined; accordingly, a different FIR is assigned to each bond, which is then used to compute a weighted average, the MEFIR. Concretely, an ion at the centre of a uniform polyhedron can be described as a sphere whose dimension, FIR, is directly

[1] Uniform polyhedra include regular, quasi-regular and semi-regular polyhedra, *i.e.* polyhedra in which the distances from the centre to the vertices are all identical.

electronic reprint

related to the ionic radius, $R(i)$. For non-uniform polyhedra, instead, the ionic radius shows a dependence on the direction, which leads to a polyhedral shape for the atomic basins (Pendás *et al.*, 1998). The computation of MEFIR corresponds to assigning to the ion a spherical basin whose radius is a weighted average of the ionic radius for each direction. MEFIR is calculated through a convergent iterative process

$$
\begin{aligned}
&{}^{n}\mathrm{MEFIR}(ij \rightarrow r) \\
&= \frac{\sum_s \sum_L \mathrm{FIR}(ij \rightarrow rs)_L \cdot \exp\left\{1 - \left[\frac{\mathrm{FIR}(ij\rightarrow rs)_L}{{}^{n-1}\mathrm{MEFIR}(ij\rightarrow r)}\right]^6\right\}}{\sum_s \sum_L \exp\left\{1 - \left[\frac{\mathrm{FIR}(ij\rightarrow rs)_L}{{}^{n-1}\mathrm{MEFIR}(ij\rightarrow r)}\right]^6\right\}}, \quad (2)
\end{aligned}
$$

where n is the number of iterations and where the starting value, ${}^{0}\mathrm{MEFIR}(ij \rightarrow r)$, is simply $\mathrm{FIR}(ij \rightarrow rs)_1$. The exponential term is responsible for the asymptotic decrease of the contribution of each FIR with increasing bond distance. MEFIR gives a quantitative meaning to the *rule of mutual influence* (Beck, 2014) of different cations on their seeming size and polarity, according to which the size of an ion depends on the chemical relations with its neighbours.

The concepts of FIR and MEFIR have been introduced for ionic bonds but they do also apply to polar bonds. According to Pauling's (1960) classification, chemical bonds can be divided into ionic, polar and non-polar depending on the difference of the electronegativity of the bonded atoms, this difference being respectively higher than 1.7, between 0.4 and 1.7, and lower than 0.4. For polar bonds, one could simply use covalent radii instead of ionic radii in equation (1): $\mathrm{FIR}(ij \rightarrow rs)_1$ would then correspond to the covalent radius for bond order 1, or be smaller than for higher bond orders. The CHARDI treatment is actually independent of the type of radii chosen.

FIR and MEFIR clearly aim at treating with a spherical model atoms which are not necessarily spherical. The purpose is to keep the description of a crystal structure as simple as possible, with nevertheless some consideration of the effect of the environment in which each atom is embedded. In the same line, the classical definition of the coordination number of an atom as 'the number of other atoms directly linked to that specified atom' (IUPAC, 1997) becomes less and less satisfactory with the distribution of bond distances over a large interval, from uniform polyhedra to cavities which can hardly be recognized as polyhedra, like in the typical example of alkaline metals showing a very irregular coordination. These considerations led Hoppe (1970) to call the coordination number an 'inorganic chameleon' and generalize it to a function of the weighted average of bond distances which he called the effective coordination number, ECoN (Hoppe, 1979). A weighted mean distance ${}^{n}d(ij \rightarrow r)$ is computed through a convergent iterative process similar to that used to compute MEFIR

$$
{}^{n}d(ij \rightarrow r) = \frac{\sum_s \sum_L d(ij \rightarrow rs)_L \cdot \exp\left\{1 - \left[\frac{d(ij\rightarrow rs)_L}{{}^{n-1}d(ij\rightarrow r)}\right]^6\right\}}{\sum_s \sum_L \cdot \exp\left\{1 - \left[\frac{d(ij\rightarrow rs)_L}{{}^{n-1}d(ij\rightarrow r)}\right]^6\right\}}, \quad (3)
$$

with ${}^{0}d(ij \rightarrow r) = d(ij \rightarrow rs)_1$. The shortest PC—V distance in each polyhedron is used as a *normalizing parameter* at the zeroth stage of the iteration, to be replaced by the weighted average until convergence is reached. This exponential term is a measure of the bond strength and has been called the *bond weight* (Nespolo *et al.*, 2001) ${}^{n}w(ij \rightarrow rs)$

$$
{}^{n}w(ij \rightarrow rs)_L = \exp\left\{1 - \left[\frac{d(ij \rightarrow rs)_L}{{}^{n}d(ij \rightarrow r)}\right]^6\right\}. \quad (4)
$$

Equation (3) can thus be rewritten as

$$
{}^{n}d(ij \rightarrow r) = \frac{\sum_s \sum_L d(ij \rightarrow rs)_L \cdot {}^{n-1}w(ij \rightarrow rs)_L}{\sum_s \sum_L \cdot {}^{n-1}w(ij \rightarrow rs)_L}. \quad (3')
$$

The sum over the bond weights gives the $\mathrm{ECoN}(ij \rightarrow r)$

$$
\mathrm{ECoN}(ij \rightarrow r) = \sum_s \sum_L {}^{n}w(ij \rightarrow rs)_L. \quad (5)
$$

If a structure contains only one type of V atom, one speaks of homoligand polyhedra (Mohri, 2000): in that case, $r = 1$ and a unique $\mathrm{ECoN}(ij)$ for each polyhedron is obtained from equation (5).

ECoN, as a generalization of the classical coordination number, is a *real* number that has to become equal to the integer coordination number for uniform polyhedra. This is the condition imposed to obtain the *contraction parameter* 6 in the definition of the weight $w(ij \rightarrow rs)$ as well as of MEFIR. It was in fact obtained by finding the highest value giving an ECoN equal to the number of first neighbours in the structure of simple metals, where a clear separation between a first and a second coordination sphere exists (Hoppe, 1979). For the very special case of hydrogen bonds, where the ratio of two short distances (donor–H and H–acceptor) with a high relative gap made the weight $w(ij \rightarrow rs)$ for the second bond negligible, a revised contraction parameter of 1.6 has been introduced (Nespolo *et al.*, 2001).

Equations (3) and (4) can be rewritten in terms of FIR and MEFIR. In fact, by replacing $d(ij\rightarrow rs)_L$ with $\mathrm{FIR}(ij\rightarrow rs)_L.[R(i)+R(r)]/R(i)$ we obtain immediately the following equivalences.

electronic reprint

$$
{}^{1}d(ij\rightarrow r)=\frac{\sum_s\sum_L d(ij\rightarrow rs)_L\cdot\exp\left\{1-\left[\frac{d(ij\rightarrow rs)_L}{d(ij\rightarrow rs)_1}\right]^6\right\}}{\sum_s\sum_L\cdot\exp\left\{1-\left[\frac{d(ij\rightarrow rs)_L}{d(ij\rightarrow rs)_1}\right]^6\right\}}=
$$

$$
\frac{\sum_s\sum_L \mathrm{FIR}(ij\rightarrow rs)_L\frac{R(i)+R(r)}{R(i)}\cdot\exp\left\{1-\left[\frac{\mathrm{FIR}(ij\rightarrow rs)_L\frac{R(i)+R(r)}{R(i)}}{\mathrm{FIR}(ij\rightarrow rs)_1\frac{R(i)+R(r)}{R(i)}}\right]^6\right\}}{\sum_s\sum_L\cdot\exp\left\{1-\left[\frac{\mathrm{FIR}(ij\rightarrow rs)_L\frac{R(i)+R(r)}{R(i)}}{\mathrm{FIR}(ij\rightarrow rs)_1\frac{R(i)+R(r)}{R(i)}}\right]^6\right\}}=
$$

$$
\frac{\sum_s\sum_L \mathrm{FIR}(ij\rightarrow rs)_L\cdot\exp\left\{1-\left[\frac{\mathrm{FIR}(ij\rightarrow rs)_L}{\mathrm{FIR}(ij\rightarrow rs)_1}\right]^6\right\}}{\sum_s\sum_L\cdot\exp\left\{1-\left[\frac{\mathrm{FIR}(ij\rightarrow rs)_L}{\mathrm{FIR}(ij\rightarrow rs)_1}\right]^6\right\}}\frac{R(i)+R(r)}{R(i)}=
$$

$$
{}^{1}\mathrm{MEFIR}(ij\rightarrow r)\frac{R(i)+R(r)}{R(i)} \qquad (6)
$$

and by iteration

$$
{}^{n}d(ij\rightarrow r)={}^{n}\mathrm{MEFIR}(ij\rightarrow r)\frac{R(i)+R(r)}{R(i)} \qquad (7)
$$

so that the bond weight too can be rewritten in terms of FIR and MEFIR

$$
\begin{aligned}
{}^{n}w(ij\rightarrow rs)_L&=\exp\left\{1-\left[\frac{d(ij\rightarrow rs)_L}{{}^{n}d(ij\rightarrow r)}\right]^6\right\}\\
&=\exp\left\{1-\left[\frac{\frac{R(i)+R(r)}{R(i)}\cdot\mathrm{FIR}(ij\rightarrow rs)_L}{\frac{R(i)+R(r)}{R(i)}\cdot{}^{n}\mathrm{MEFIR}(ij\rightarrow r)}\right]^6\right\}\\
&=\exp\left\{1-\left[\frac{\mathrm{FIR}(ij\rightarrow rs)_L}{{}^{n}\mathrm{MEFIR}(ij\rightarrow r)}\right]^6\right\}. \qquad (8)
\end{aligned}
$$

Although the formulae look exactly equivalent, the results significantly differ in the case of heteroligand polyhedra. If r takes only one value (homoligand polyhedra), equations (4) and (8) give exactly the same result. If instead r takes multiple values, equation (4) has to be computed separately for each r so that each heteroligand polyhedron is divided into homoligand subpolyhedra, treated independently, while this is not the case for equation (8). In fact, by using the bond lengths in equations (3)–(5) one automatically selects a different normalizing parameter (minimal distance) for each type of V atom: it would make no sense to normalize bond lengths of a V atom with respect to the shortest bond length of a *different* V atom having in general a different size. It would also make no sense to define a unique weighted mean distance ${}^{n}d(ij)$ by making r in ${}^{n}d(ij\rightarrow r)$ variable over all the V atoms coordinated by the same PC atom because the corresponding bond distances can be significantly different so that global average would overestimate bonds with smaller V atoms and underestimate bonds with larger V atoms. Accordingly, $\mathrm{ECoN}(ij\rightarrow r)$, equation (5), is defined unambiguously for each homoligand subpolyhedron, and the resulting $\mathrm{ECoN}(ij\rightarrow r)$ are then summed up to obtain $\mathrm{ECoN}(ij)$

$$
\mathrm{ECoN}(ij)=\sum\nolimits_r\mathrm{ECoN}(ij\rightarrow r)=\sum\nolimits_r\sum\nolimits_s\sum\nolimits_L{}^{n}w(ij\rightarrow rs)_L \qquad (9)
$$

thus ignoring the effect of the size of the different V atoms at this stage.

By using FIR, a global ${}^{n}\mathrm{MEFIR}(ij)$ for each PC atom can be defined because ${}^{n}\mathrm{MEFIR}(ij\rightarrow r)$ does not change significantly as a function of r

$$
{}^{n}\mathrm{MEFIR}(ij)=\frac{\sum_r\sum_s\sum_L \mathrm{FIR}(ij\rightarrow rs)_L\cdot\exp\left\{1-\left[\frac{\mathrm{FIR}(ij\rightarrow rs)_L}{{}^{n-1}\mathrm{MEFIR}(ij)}\right]^6\right\}}{\sum_r\sum_s\sum_L\exp\left\{1-\left[\frac{\mathrm{FIR}(ij\rightarrow rs)_L}{{}^{n-1}\mathrm{MEFIR}(ij)}\right]^6\right\}} \qquad (2')
$$

$$
{}^{n}w(ij\rightarrow rs)_L=\exp\left\{1-\left[\frac{\mathrm{FIR}(ij\rightarrow rs)_L}{{}^{n}\mathrm{MEFIR}(ij)}\right]^6\right\} \qquad (8')
$$

Equation (2′) allows treating all the PC—V distances in a polyhedron at once; this however leads to neglecting the differences between the various V atoms. In other words, it corresponds to replacing each V atom with a dimensionless charged point. While this does make sense in the calculation of $\mathrm{ECoN}(ij)$, which simply gives a measure of the number of coordinated V atoms weighted by the respective bond distances, it would prevent any charge distribution analysis. In fact, although every V atom retains its charge, the relation between the bond distance and the strength of the bond would be lost. There is, however, one aspect in which the use of FIR and MEFIR instead of the individual and average distances presents a clear advantage.

In a structure built on homoligand polyhedra, every PC(ij) is bonded to V(1s) for some s and the minimal PC—V distance, $d(ij\rightarrow 1s)_1$, obviously corresponds to a chemical bond between the two atoms. On the other hand, in a structure containing heteroligand polyhedra not all the PC(ij) are necessarily bonded to every V(rs). In other words, $d(ij\rightarrow rs)_1$ for some r may correspond to a non-bonded contact. If the distances are used directly, then $d(ij\rightarrow rs)_1$ is scaled to itself in the first step of the calculation of the average distance, $d(ij\rightarrow r)$, and to avoid considering non-bonded contacts as chemical bonds one needs an external criterion, like the sum of the radii scaled by an expansion factor to allow some tolerance. This is the somehow empirical solution we had adopted in the previous version of the algorithm. If FIR and MEFIR are used instead, each polyhedron is treated as a homoligand at this stage and the risk of counting non-bonded contacts as chemical bonds is avoided.

Concretely, in the analysis of the coordination polyhedra, a first step is performed in term of FIR and MEFIR, equations (2′) and (8′), to discriminate between bonding and non-bonding contacts; then the calculation is repeated by using the distances to treat each coordination sub-polyhedron separately.

electronic reprint

3. Charge distribution

Once ECoN($ij \rightarrow r$) has been obtained through equation (5), it is distributed among all the bonds around the PC atom defining a homoligand subpolyhedron, obtaining in this way the contribution by each V atom to ECoN itself

$$\Delta\mathrm{ECoN}(ij \rightarrow rs) = \frac{\sum_L {}^n w(ij \rightarrow rs)_L}{\mathrm{ECoN}(ij \rightarrow r)}. \qquad (10)$$

In a correctly refined and well balanced structure, the distribution of ECoN among the PC-—V bonds should sum up to some expected value for both PC(ij) and V(rs). As an expected value, the formal charge $q(ij)$ is used as a *scaling parameter* applied to ΔECoN

$$\Delta q(ij \rightarrow rs) = \Delta\mathrm{ECoN}(ij \rightarrow rs) q(ij) \qquad (11)$$

As discussed above, a single weighted mean distance ${}^n d(ij)$ for each PC-atom cannot be defined, but only weighted mean distances ${}^n d(ij \rightarrow r)$ for each PC—V atom pairs. To take into account the presence of different V atoms in heteroligand polyhedra, a scale factor $F(ij \rightarrow r)$ was introduced in equation (11) (Nespolo *et al.*, 2001). Then, summing the $\Delta q(ij \rightarrow rs)$ on the PC atoms about a V atom, one should obtain the expected 'charge' of the V atom itself

$$Q(rs) = -\sum_i \sum_j \Delta q(ij \rightarrow rs) \frac{h(ij)}{h(rs)}. \qquad (12)$$

The ratio of the multiplicities of the respective Wyckoff positions, $h(ij)/h(rs)$, is introduced to avoid counting multiple contributions when a bond connects atoms on Wyckoff positions with different multiplicities.

A similar distribution is repeated the other way round and summed up on the V atoms about a PC atom. This time, however, instead of using $q(rs)$ as the scaling parameter, in a perfectly symmetrical way, the ratio $q(rs)/Q(rs)$ for the V(rs) bonded to PC(ij) is used

$$\begin{aligned} Q(ij) &= \left[\sum_r \sum_s \Delta\mathrm{ECoN}(ij \rightarrow rs) \frac{q(rs)}{Q(rs)}\right] q(ij) \\ &= \sum_r \sum_s \Delta q(ij \rightarrow rs) \frac{q(rs)}{Q(rs)}. \end{aligned} \qquad (13)$$

If $q(rs)/Q(rs) = 1$ for each r and s, then the bracket in equation (13) goes to 1 (it becomes the sum of the fractions of ECoN about each PC atom) and thus $Q(ij) = q(ij)$. This shows that in a structure correctly solved and perfectly valence-balanced the distribution of ECoN scaled by the formal charges gives back these charges. On the other hand, when a structure has developed some structural tensions, its V atoms may not be perfectly balanced but the distribution of this unbalance, measured by the ratio $q(rs)/Q(rs)$, should give back the expected formal charges on the PC atoms, otherwise the whole set of coordination polyhedra would be unbalanced and the structure would be unstable. In other words, CHARDI possesses an internal criterion to evaluate the quality of its analysis: the ratio $q(ij)/Q(ij)$ for the PC atoms. When this ratio is reasonably close to 1 for all the PC atoms, then the analysis of the connectivity can be approached by the study of $Q(rs)$, which diverge from $q(rs)$ proportionally to the structural strains inside the structure. One speaks of the *over–under-bonding (OUB) effect* (Nespolo *et al.*, 1999, 2001). Quite obviously, in the trivial case of a structure containing only one type of V atom there is nothing to distribute, $Q(rs)$ is identical to $q(rs)$ and the CHARDI analysis simply does not give any information.

As an overall measure of the agreement between q and Q for the whole sets of PC atoms and of V atoms, the *mean absolute percentage deviation* (MAPD) is used

$$\mathrm{MAPD} = \frac{100}{N} \sum_{i-1}^{N} \left| \frac{q_i - Q_i}{q_i} \right|. \qquad (14)$$

The generalization of the approach to anion-centred structures and a wider set of tests has prompted us to reconsider the solution. Indeed, the scale factors adopted in the previous version were computed in an iterative way assuming that a real OUB effect affects mainly the anionic charges of each single anion, but without grossly modifying the total charge of each type of anion. However, if a single crystallographic type of anion occurs in the structure (*i.e.* $s = 1$ for some r) this procedure may force the expected charge on that anion. We have therefore introduced a new route to treat structures in a more correct manner with heteroligand polyhedra.

4. A new route to heteroligand polyhedra

In the case of the homoligand polyhedra ($r = 1$), every PC atom distributes its charge to all the V atoms bonded to it, in an inverse proportion to the bond length. In a heteroligand polyhedra ($r > 1$), each PC atom distributes a fraction of its charge to each homoligand subpolyhedron. This fraction depends on the relative distances: V atoms closer to the PC atom receive a larger fraction than V atoms farther from it. The problem is how to define this fraction. This is straightforward for structures which are built by homoligand polyhedra in one of the two possible descriptions (cation-centred or anion-centred), while it requires a convergence algorithm when a structure is built by heteroligand polyhedra in both descriptions.

4.1. Structures built by homoligand polyhedra in one description

If a structure contains only one chemical species of cations or of anions, the calculation is straightforward. The single type of atom (cation or anion) is first assigned to V atoms and the computation described above is performed. Next, the fraction of $Q(ij)$ from each V atom is calculated by a simple modification of equation (13)

electronic reprint

Table 1
Bond distances d (Å), FIR (Å) and bond weights w of laurelite (Merlino *et al.*, 1996) in the anion-centred description, where the structure is built by homoligand polyhedra.

PC(ij)	$q(ij)$	$h(ij)$	$V(rs)$	$q(rs)$	$h(rs)$	$d(ij \rightarrow rs)$	FIR($ij \rightarrow rs$)	$w(ij \rightarrow rs)$
Cl 1	−1	1	Pb 1	2	3	3.1597 × 2	1.759 × 2	1.001 × 2
			Pb 1	2	3	3.1601 × 2	1.759 × 2	1.000 × 2
			Pb 1	2	3	3.1605 × 2	1.759 × 2	0.999 × 2
Cl 2	−1	1	Pb 2	2	3	3.2103 × 2	1.787 × 2	1.001 × 2
			Pb 2	2	3	3.2108 × 2	1.787 × 2	1.000 × 2
			Pb 2	2	3	3.2111 × 2	1.787 × 2	0.999 × 2
F 1	−1	3	Pb 1	2	3	2.4723	1.146	1.173
			Pb 2	2	3	2.5361 × 2	1.176 × 2	1.021 × 2
			Pb 1	2	3	2.7215	1.262	0.610
F 2	−1	3	Pb 1	2	3	2.4405 × 2	1.132 × 2	1.179 × 2
			Pb 2	2	3	2.6049	1.208	0.790
			Pb 2	2	3	2.7048	1.254	0.578
F 3	−1	3	Pb 2	2	3	2.4717	1.146	1.490
			Pb 3	2	1	2.7500 × 2	1.275 × 2	0.869 × 2
			Pb 1	2	3	2.9885 × 2	1.386 × 2	0.416 × 2
F 4	−1	3	Pb 1	2	3	2.3998	1.113	1.206
			Pb 3	2	1	2.4299	1.127	1.132
			Pb 2	2	3	2.5991 × 2	1.205 × 2	0.732 × 2

Table 2
MEFIR (Å), average distance d (Å), ECoN and computed charges of laurelite in the anion-centred description.

PC(ij)	MEFIR(ij)	$d(ij)$	ECoN(ij)	Q	$V(rs)$	Q	$\Delta Q(i \rightarrow rs)$	
Cl 1	1.789	3.160	6.00	−1.02	Pb 1	1.95	Pb1—Cl	0.341
Cl 2	1.787	3.211	6.00	−1.01	Pb 2	1.99	Pb1—F	1.659
F 1	1.180	2.545	3.83	−1.01	Pb 3	2.18	Pb2—Cl	0.336
F 2	1.166	2.515	3.73	−1.02			Pb2—F	1.664
F 3	1.247	2.691	4.06	−0.97			Pb3—Cl	–
F 4	1.152	2.484	3.80	−0.99			Pb3—F	2.0
MAPD				1.8		2.5		

$$\Delta Q(i \rightarrow rs) = \sum_j \Delta q(ij \rightarrow rs) \frac{q(rs)}{Q(rs)} \frac{h(ij)}{h(rs)} = \frac{\sum_j \Delta \mathrm{ECoN}(ij \rightarrow rs) h(ij) q(ij)}{Q(rs) h(rs)} q(rs). \quad (15)$$

The summation here is over j, *i.e.* the crystallographic type of PC atom, rather than r and s. The result is thus the fraction of the formal charge that each V atom (of chemical species r and crystallographic type s) shares with the ith chemical species of the PC atom. The role of PC atoms and V atoms is then exchanged so that equation (15) gives in the next step $\Delta Q(ij \rightarrow r)$, *i.e.* the fraction that each PC atom (V atom in the previous step) shares with each chemical species of the V atom (PC atom in the previous step)

$$\Delta Q(ij \rightarrow r) = -\Delta Q(i \rightarrow rs), \quad (16)$$

with the exchange $r \rightarrow i, j \rightarrow s, i \rightarrow r$. $\Delta Q(ij \rightarrow r)$ is then used instead of $q(ij)$ in equation (13), which is replaced by equation (17)

$$Q(ij) = \sum_r \sum_s \Delta \mathrm{ECoN}(ij \rightarrow rs) \frac{q(rs)}{Q(rs)} \Delta Q(ij \rightarrow r). \quad (17)$$

Clearly, if $r = 1$, equation (17) reduces to equation (13).

Table 3
Bond distances d (Å), FIR (Å) and bond weights of laurelite in the cation-centred description, where the structure is built by heteroligand polyhedra.

PC(ij)	$q(ij)$	$h(ij)$	$V(rs)$	$q(rs)$	$h(rs)$	$d(ij \rightarrow rs)$	FIR($ij \rightarrow rs$)	$w(ij \rightarrow rs)$
Pb 1	2	3	Cl 1	−1	1	3.1605 × 2	1.401 × 2	1.000 × 2
			F 4	−1	3	2.3998	1.287	1.217
			F 2	−1	3	2.4405 × 2	1.309 × 2	1.117 × 2
			F 1	−1	3	2.4723	1.326	1.040
			F 1	−1	3	2.7215	1.460	0.492
			F 3	−1	3	2.9885 × 2	1.603 × 2	0.136 × 2
Pb 2	2	3	Cl 2	−1	1	3.2108 × 2	1.423 × 2	1.000×2
			F 3	−1	3	2.4717	1.326	1.225
			F 1	−1	3	2.5361 × 2	1.360 × 2	1.073 × 2
			F 4	−1	3	2.5991 × 2	1.394 × 2	0.926 × 2
			F 2	−1	3	2.6049	1.397	0.912
			F 2	−1	3	2.7048	1.451	0.692
Pb 3	2	1	F 4	−1	3	2.4299 × 3	1.303 × 3	1.353 × 3
			F 3	−1	3	2.7500 × 6	1.475 × 6	0.627 × 6

4.2. Structures built by heteroligand polyhedra in both descriptions

When a structure contains heteroligand polyhedra in both descriptions, we miss the starting point to compute equation (15). The problem is solved with an iterative procedure in which the starting value of $\Delta Q(ij \rightarrow r)$ in equation (16) is assigned as a function of $\mathrm{ECoN}(ij \rightarrow r)/\mathrm{ECoN}(ij)$

$$\Delta Q(ij \rightarrow r) = q(ij) \frac{\mathrm{ECoN}(ij \rightarrow r)}{\mathrm{ECoN}(ij)} \quad (16')$$

Equation (16′) corresponds to Pauling's definition of bond strength ($s = Q/N$, N being the classical integer coordination number) applied to each sub-polyhedron. From the second step equations (15) and (16) can be used directly and the role of PC and V atoms is swapped back and forth between cations and anions until the same values of $\Delta Q(ij \rightarrow r)$ are obtained in each description, meaning that convergence has been obtained.

5. Case analysis

In this section we analyse a few cases of charge distribution applied to crystal structures and show that when a Madelung-type description is possible then CHARDI provides a powerful tool of structure validation. Unsatisfactory results on correctly refined structures actually originate from the departure of the structure under investigation from the simple Madelung-type model. All the calculations have been performed with a new version of the CHARDI software (Nespolo *et al.*, 2001), which is available at http://www.crystallography.fr/chardi.

5.1. Laurelite: a structure based on anion-centred poyhedra

The structure of laurelite, $Pb_7Cl_2F_{12}$, was reported by Merlino *et al.* (1996) and is based on homoligand anion-centred polyhedra but heteroligand cation-centred polyhedra. The analysis starts with the homoligand description and is given in Table 1. The results of the charge distribution analysis

electronic reprint

Table 4
MEFIR (Å), average distance d (Å), ECoN and computed charges of laurelite in the cation-centred description.

PC(ij)		$V(r)$	MEFIR ($ij \rightarrow r$)	$d(ij \rightarrow r)$	ECoN ($ij \rightarrow r$)	ECoN(ij)	Q	r	s	Q
Pb	1	Cl	1.401	3.160	2.00	7.25	1.90	Cl	1	−1.02
		F	1.334	2.489	5.25			Cl	2	−1.01
Pb	2	Cl	1.423	3.211	2.00	8.83	2.02	F	1	−1.01
		F	1.377	2.567	6.83			F	2	−1.10
Pb	3	Cl	–	–	–	7.82	2.24	F	3	−0.71
		F	1.383	2.580	7.82			F	4	−1.18
MAPD							4.1			12.6

(Table 2) are satisfactory, showing only a small OUB effect. The values of $\Delta Q(i \rightarrow rs)$ in the last column of Table 2 are used to compute the charge distribution of the cation-centred description (coordination in Table 3) and the results are shown in Table 4. They are imperfectly satisfactory for the PC atoms and definitely unsatisfactory for the V atoms. The presence of a very large cation (lead in this case) is one of the conditions listed in Eon & Nespolo (2015) for a possible preferable description of the structure as anion-centred: this is likely the reason why the roles of cations and anions are exchanged with respect to the classical, cation-centred description, with large cations building the bulk of the framework and the anions filling the holes of it. Furthermore, the structure representation shows that in the anion-centred description (Fig. 1) well defined coordination polyhedra appear: almost perfectly regular $ClPb_6$ trigonal prisms, slightly deformed FPb_4 tetrahedra for F1, F2 and F4, and a FPb_5 polyhedron which can be described as a deformed square pyramid with two longer (3.98 Å) and two shorter (3.83 Å) basal Pb—Pb edges. This coordination is much more regular than that based on the cations (Fig. 2). However, as we are going to see in the case of crocoite, a regular set of polyhedra cannot exist in a hetero-ligand description with V atoms of largely different size and valence, yet the structure may still be correctly described as anion-centred.

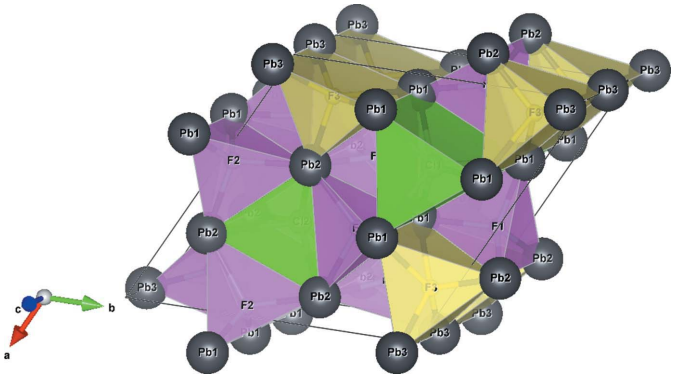

Figure 1
The structure of laurelite (Merlino *et al.*, 1996) in the anion-centred description. The two Cl atoms are at the centre of trigonal prisms, F1, F2 and F4 of tetrahedra, F3 of a square pyramid (polyhedra are differentiated by the colour). All the coordination polyhedra, especially those of fluorine are actually slightly distorted. Figure drawn using *VESTA* (Momma & Izumi, 2011).

5.2. $Y_2Cu_2O_5$: a structure based on oxygen-centred polyhedra

Delafossite compounds, from the name of the prototype mineral $CuFeO_2$, belong to a family of ternary oxides with the general formula ABO_2, where the A cation (typically Pd, Pt, Cu or Ag) is linearly coordinated to two oxygen ions and the B cation (Ga, In, Al, Fe, Co, Y, La, Nd, Eu) is located in distorted edge-sharing BO_6 octahedra. The oxygen ion is in pseudo-tetrahedral coordination with one A and three B cations (Marquardt *et al.*, 2006). Delafossites typically occur in two polytypes: 2H and 3R, with space-group types $P6_3/mmc$ and $R\bar{3}m$, respectively, containing only one type of anion. The CHARDI algorithm does not convey any information when applied to the cation-centred description, because when only

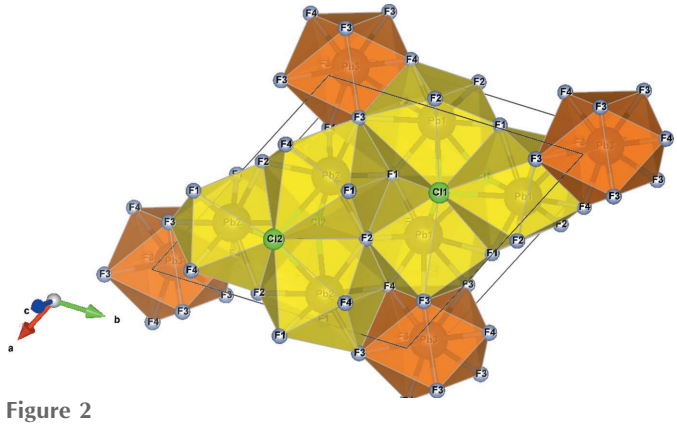

Figure 2
The structure of laurelite in the cation-centred description. Pb1 and Pb2 coordinate two Cl and seven F in a rather irregular polyhedron (yellow), whereas Pb3 coordinates eight F in a more regular 2 + 6 polyhedron (orange). Pb1 shares faces with Pb1 and Pb3, edges with Pb2; Pb2 shares faces with Pb2, edges with Pb1 and Pb3; Pb3 shares faces with Pb1 and Pb3, edges with Pb2. Figure drawn using *VESTA*.

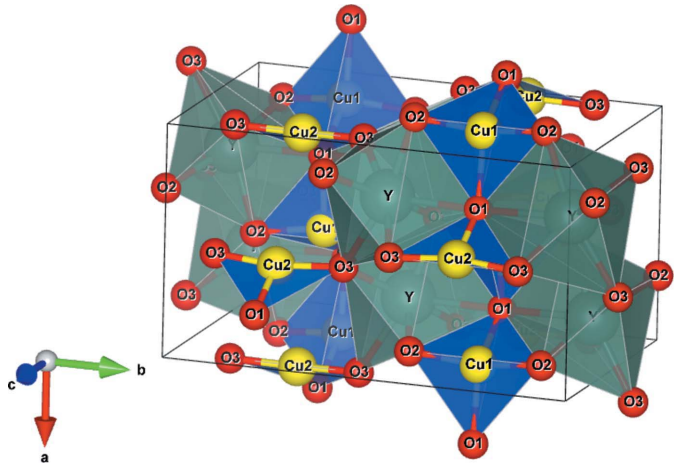

Figure 3
The structure of delafossite $Y_2Cu_2O_5$ (Van Tendeloo *et al.*, 2001) in the cation-centred description. The Cu atoms are located on the edge of a disphenoid (Cu1) or of a triangle (Cu2) which correspond to the dumbbell in the prototype delafossite, where the metal has linear coordination. Figure drawn using *VESTA*.

electronic reprint

Table 5
Bond distances d (Å), FIR (Å) and bond weights of Y_2CuO_5 (Van Tendeloo *et al.*, 2001) in the cation-centred description, where the structure is built by homoligand polyhedra.

PC(ij)	$q(ij)$	$h(ij)$	$V(rs)$	$q(rs)$	$h(rs)$	$d(ij \rightarrow rs)$	FIR($ij \rightarrow rs$)	$w(ij \rightarrow rs)$
Y 1 3	8	O 2	−2	8	2.2357	1.033	1.241
		O 2	−2	8	2.2460	1.038	1.214
		O 3	−2	8	2.3051	1.065	1.060
		O 2	−2	8	2.3420	1.083	0.965
		O 3	−2	8	2.3789	1.100	0.871
		O 3	−2	8	2.4471	1.131	0.706
		O 1	−2	8	2.5632	1.848	0.458
Cu 1 2	4	O 2	−2	8	1.8679 × 2	0.691 × 2	1.206 × 2
		O 1	−2	4	2.0627	0.763	0.622
		O 1	−2	4	2.0759	0.768	0.588
Cu 2 2	4	O 3	−2	8	1.8073 × 2	0.668 × 2	1.074 × 2
		O 1	−2	4	1.8898	0.699	0.807

Table 6
MEFIR (Å), average distance d (Å), ECoN and computed charges of Y_2CuO_5 in the cation-centred structure.

PC(ij)	MEFIR(ij)	$d(ij)$	ECoN(ij)	Q	$V(rs)$	Q	$\Delta Q(i \rightarrow rs)$
Y 1	1.076	2.328	6.52	2.91	O 1	−1.64	O1—Y −0.516
Cu 1	0.715	1.934	3.62	2.01	O 2	−2.24	O1—Cu −1.484
Cu 2	0.677	1.830	2.95	2.17	O 3	−1.94	O2—Y −1.406
							O2—Cu −0.594
							O3—Y −1.521
							O3—Cu −0.749
MAPD				3.6		9.6	

one type of V atom is present in the structure, there is nothing to distribute and $Q(ij)$ necessarily matches $q(ij)$, as discussed in §3. The anion-centred description gives a perfect match too.

Table 7
Bond distances d (Å), FIR (Å) and bond weights of Y_2CuO_5 in the anion-centred description, where the structure is built by heteroligand polyhedra.

PC(ij)	$q(ij)$	$h(ij)$	$V(rs)$	$q(rs)$	$h(rs)$	$d(ij \rightarrow rs)$	FIR($ij \rightarrow rs$)	$w(ij \rightarrow rs)$
O 1	−2	4	Y 1 3	8	2.5632 × 2	1.378 × 2	1.000 × 2
			Cu 2 2	8	1.8898	1.191	1.290
			Cu 1 2	8	2.0627	1.300	0.770
			Cu 1 2	8	2.0759	1.308	0.734
O 2	2	8	Y 1 3	8	2.2357	1.202	1.087
			Y 1 3	8	2.2460	1.208	1.059
			Y 1 3	8	2.3420	1.259	0.809
			Cu 1 2	8	1.8679	1.177	1.000
O 3	2	8	Y 1 3	8	2.3051	1.240	1.160
			Y 1 3	8	2.3789	1.279	0.972
			Y 1 3	8	2.4471	1.316	0.803
			Cu 1 2	8	1.8073	1.139	1.000

Delafossites of the type $LaCuO_2$ and $YCuO_2$ are also known to easily intercalate extra O atoms, which tend to adopt an ordered arrangement within the CuO_x plane and give rise to derived structures $LnCuO_{2+x}$ (Ln = La or Y) consisting of a planar layer of A cations forming additional bonds with respect to the linear coordination in the prototype structure, and a layer of edge-sharing BO_6 octahedra flattened with respect to the **c** axis. The structure of $Y_2Cu_2O_5$, corresponding to x = 0.5, was reported by Van Tendeloo *et al.* (2001) and is shown in Figs. 3 (cation centred) and 4 (anion centred). In the cation-centred description, the Cu atoms are located on the edge of a disphenoid (Cu1) or of a triangle (Cu2) which corresponds to the dumbbell in the prototype delafossite, where the metal would have linear coordination. In the anion-centred description, the O atoms are at the centre of O[Y_3Cu] pseudo-tetrahedra (O2, O3; red in the figure) and of

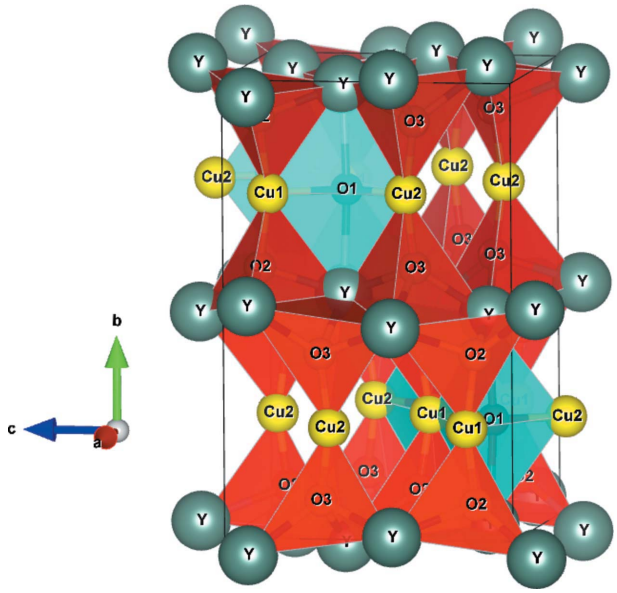

Figure 4
The structure of delafossite $Y_2Cu_2O_5$ in the anion-centred description. The O atoms are at the centre of O[Y_3Cu pseudo-tetrahedra] (O2, O3; red in the figure) or of O1[Y_2Cu_3] pseudo-trigonal bipyramids (cyan in the figure), in corner- and edge-sharing topology in which pairs of corner-sharing bipyramids are alternatively occupied and empty. Figure drawn using *VESTA*.

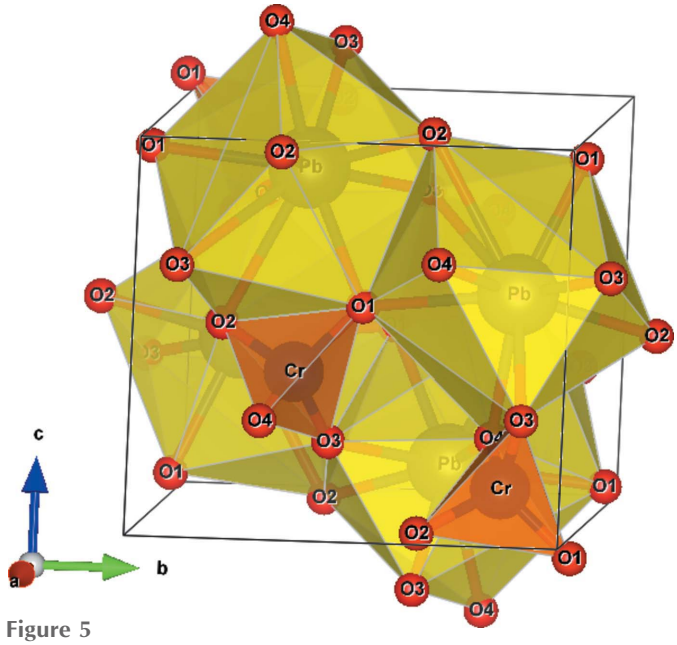

Figure 5
The structure of crocoite (Effenberger & Pertlik, 1986) in the cation-centred description. Chromium has an almost regular tetrahedral coordination, while lead is coordinated by nine O atoms spread on a large interval of distances. Figure drawn using *VESTA*.

electronic reprint

Table 8
MEFIR (Å), average distance d (Å), ECoN and computed charges of Y_2CuO_5 in the anion-centred structure.

PC(ij)		$V(r)$	MEFIR ($ij \rightarrow r$)	$d(ij \rightarrow r)$	ECoN ($ij \rightarrow r$)	ECoN(ij)	Q	r	s	Q
O	1	Y	1.378	2.563	2.00	4.79	−1.96	Y	1	2.91
		Cu	1.250	1.985	2.79			Cu	1	1.99
O	2	Y	1.220	2.268	2.95	3.95	−2.04	Cu	2	2.18
		Cu	1.177	1.868	1.00					
O	3	Y	1.273	2.368	2.94	3.94	−1.97			
		Cu	1.139	1.807	1.00					
MAPD							1.8			3.9

Table 9
Bond distances d (Å), FIR (Å) and bond weights of crocoite (Effenberger & Pertlik, 1986) in the cation-centred description, where the structure is built by homoligand polyhedra.

PC(ij)	$q(ij)$	$h(ij)$	$V(rs)$	$q(rs)$	$h(rs)$	$d(ij \rightarrow rs)$	FIR($ij \rightarrow rs$)	$w(ij \rightarrow rs)$
Pb 1	2	4	O 3	−2	4	2.5313	1.325	1.224
			O 2	−2	4	2.5531	1.337	1.174
			O 4	−2	4	2.5715	1.347	1.131
			O 1	−2	4	2.5913	1.357	1.085
			O 3	−2	4	2.6452	1.385	0.962
			O 4	−2	4	2.6772	1.402	0.890
			O 1	−2	4	2.6882	1.408	0.865
			O 2	−2	4	2.8077	1.470	0.620
			O 2	−2	4	3.0810	1.613	0.203
Cr 1	6	4	O 4	−2	4	1.6499	0.410	1.048
			O 2	−2	4	1.6647	0.414	0.994
			O 1	−2	4	1.6671	0.414	0.986
			O 3	−2	4	1.6717	0.415	0.969

Table 10
MEFIR (Å), average distance d (Å), ECoN and computed charges of crocoite in the cation-centred description.

PC(ij)	MEFIR(ij)	$d(ij)$	ECoN(ij)	Q	$V(rs)$	Q	$\Delta Q(i \rightarrow rs)$
Pb 1	1.376	2.628	8.15	2.00	O 1	−1.96	Pb: −0.489
Cr 1	0.413	1.663	4.00	6.00			Cr: −1.511
					O 2	−1.98	Pb: −0.493
							Cr: −1.507
					O 3	−1.99	Pb: −0.539
							Cr: −1.461
					O 4	−2.07	Pb: −0.479
							Cr: −1.521
MAPD				0		0.7	

Table 11
Bond distances d (Å), FIR (Å

O1[Y_2Cu_3] pseudo-trigonal bipyramids (cyan in the figure), in corner- and edge sharing topology where pairs of corner-sharing bipyramids are alternatively occupied and empty. We may expect a better result of the CHARDI analysis in the anion-centred description, despite the presence of hetero-ligand polyhedra.

The analysis based on the homoligand description (cation-centred) is given in Table 5. The results of the charge distribution analysis (Table 6) reveal quite a large OUB effect, which is not surprising considering the very unusual coordination of the Cu atoms, which do not really form coordination polyhedra. The values of $\Delta Q(i \rightarrow rs)$ in the last column of Table 6 are used to compute the charge distribution of the anion-centred description (coordination in Table 7) and the results are shown in Table 8. As expected, the results are definitely more satisfactory because in this description the structure is really based on coordination polyhedra.

5.3. Crocoite: a structure with two possible descriptions

Crocoite, $PbCrO_4$, is an uncommon secondary mineral in lead deposits associated with chromium-bearing rocks. We use the structural data reported by Effenberger & Pertlik (1986). The Cr—O bond in chromates is usually described as consisting of two single bonds and two double bonds; however, the four Cr—O distances in crocoite (Table 9) are similar, suggesting the presence of resonance (IUPAC, 1997).

Tables 9 and 10 give the coordination details and the charge distribution results in the cation-centred description. Chromium has an almost regular tetrahedral coordination, while lead is coordinated by nine O atoms spread on a large interval of distances, corresponding to bond weights going from 1.224 to 0.203 (Fig. 5). The agreement with the input charges is excellent. The last column of Table 10 gives $\Delta Q(i \rightarrow rs)$ [equation (15)], which is used in the next step to compute the charge distribution when the structure is described as anion-centred. The corresponding coordination data are given in Table 11. Differently from the laurelite case, in crocoite the coordination polyhedra about the anions are far from regular

Table 13
Bond distances d (Å), FIR (Å) and bond weights of $K_2SeS_2O_6$ (Foust & Janickis, 1980) in the cation-centred description.

The structure is built by heteroligand polyhedra.

PC(ij)	$q(ij)$	$h(ij)$	$V(rs)$	$q(rs)$	$h(rs)$	$d(ij \rightarrow rs)$	FIR ($ij \rightarrow rs$)	$w(ij \rightarrow rs)$
S 1	6	4	Se 1	−2	4	2.2562	0.138	1.000
			O 3	−2	4	1.4387	0.130	1.032
			O 2	−2	4	1.4499	0.131	0.985
			O 1	−2	4	1.4511	0.131	0.981
S 2	6	4	Se 1	−2	4	2.2569	0.138	1.000
			O 6	−2	4	1.4359	0.130	1.029
			O 4	−2	4	1.4454	0.130	0.989
			O 5	−2	4	1.4475	0.131	0.981
K 1	1	4	O 6	−2	4	2.6551	1.581	1.193
			O 3	−2	4	2.6787	1.595	1.141
			O 5	−2	4	2.7524	1.639	0.979
			O 2	−2	4	2.7840	1.657	0.910
			O 4	−2	4	2.7950	1.664	0.887
			O 1	−2	4	2.8595	1.702	0.752
K 2	1	4	Se 1	−2	4	3.7556	1.847	1.000
			O 3	−2	4	2.6606	1.584	1.370
			O 5	−2	4	2.7706	1.649	1.134
			O 5	−2	4	2.7923	1.662	1.089
			O 1	−2	4	2.8237	1.681	1.021
			O 4	−2	4	2.8787	1.714	0.905
			O 2	−2	4	2.9548	1.759	0.751
			O 4	−2	4	2.9588	1.761	0.743
			O 1	−2	4	3.3554	1.998	0.172
			O 1	−2	4	3.4249	2.039	0.120

Table 14
Bond distances d (Å), FIR (Å) and bond weights of $K_2SeS_2O_6$ in the anion-centred description.

The structure is built by heteroligand polyhedra.

PC(ij)	$q(ij)$	$h(ij)$	$V(rs)$	$q(rs)$	$h(rs)$	$d(ij \rightarrow rs)$	FIR ($ij \rightarrow rs$)	$w(ij \rightarrow rs)$
Se 1	−2	4	S 1	6	4	2.2562	2.118	1.001
			S 2	6	4	2.2569	2.119	0.999
			K 2	1	4	3.7556	1.909	1.000
O 1	−2	4	S 1	6	4	1.4511	1.320	1.000
			K 2	1	4	2.8237	1.143	1.222
			K 1	1	4	2.8595	1.157	1.148
			K 2	1	4	3.3554	1.358	0.286
			K 2	1	4	3.4249	1.386	0.213
O 2	−2	4	S 1	6	4	1.4499	1.319	1.000
			K 1	1	4	2.7840	1.127	1.146
			K 2	1	4	2.9548	1.196	0.791
O 3	−2	4	S 1	6	4	1.4387	1.309	1.000
			K 2	1	4	2.6606	1.077	1.020
			K 1	1	4	2.6787	1.084	0.979
O 4	−2	4	S 2	6	4	1.4454	1.315	1.000
			K 1	1	4	2.7950	1.131	1.153
			K 2	1	4	2.8787	1.165	0.976
			K 2	1	4	2.9588	1.197	0.813
O 5	−2	4	S 2	6	4	1.4475	1.317	1.000
			K 1	1	4	2.7524	1.114	1.041
			K 2	1	4	2.7706	1.121	1.001
			K 2	1	4	2.7923	1.130	0.954
O 6	−2	4	S 2	6	4	1.4359	1.306	1.000
			K 1	1	4	2.6551	1.074	1.000

and the anions are off-centred, close to the cation with higher valence. All the O atoms are coordinated by one chromium and two Pb atoms, forming an irregular triangle with the oxygen closer to the chromium than to the lead; O2 has a third Pb atom with which it forms a much weaker bond defining a highly deformed tetrahedron with the oxygen close to one face (Fig. 6). Table 12 gives the charge distribution in this description: the agreement with the input charge is absolutely perfect, showing that the description of the structure as anion-centred, despite irregular coordination due to its heteroligand nature, makes perfect sense, most likely because of the large dimension of the cations.

5.4. Potassium selenotrithionate: a structure containing heteroligand polyhedra in both descriptions

The structure of $K_2SeS_2O_6$ was reported by Foust & Janickis (1980) and contains two types of cations (K^+ and S^{6+}, two crystallographic types each) and two types of anions (Se^{2-} and O^{2-}, one type of Se and six types of O). The crystal structure is built on heteroligand polyhedra in both the cation-centred and the anion-centred description, namely $S(O_3Se)$ for both S atoms, $K1O_6$ and $K2(O_9Se)$, in the cation-centred description, and $Se(S_2K)$, $O1(SK_4)$, $O2(SK_2)$, $O3(SK_2)$, $O4(SK_3)$, $O5(SK_3)$ and O6(SK), in the anion centred description. The K2—Se contact is long (3.7556 Å) yet it cannot be neglected *a priori*; in fact, FIR(K2-Se) is 1.847 Å, well within the range of FIR(K2-O) for K—O coordination, which spans the interval 1.584–2.039 Å, although the longer bond distances obviously have a smaller weight (Table 13). The anion-centred description is given in Table 14. The MEFIR, average distances and ECoN values are presented in Table 15 for both cation-centred and anion-centred descriptions.

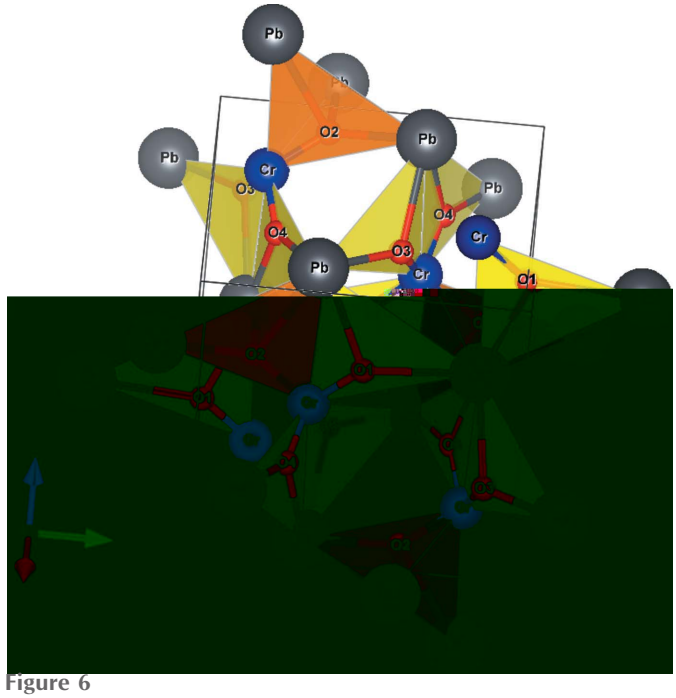

Figure 6
The structure of crocoite in the anion-centred description. All the O atoms are coordinated by one Cr and two Pb atoms, forming an irregular triangle with the oxygen closer to the chromium than to the lead; O2 has a third Pb atom with which it forms a much weaker bond defining a highly deformed tetrahedron with the oxygen close to one face. Figure drawn using *VESTA*.

electronic reprint

Table 15
MEFIR (Å), average distance d (Å) and ECoN of $K_2SeS_2O_6$.

Cation-centred description							Anion-centred description						
PC(ij)		$V(r)$	MEFIR($ij \rightarrow r$)	$d(ij \rightarrow r)$	ECoN($ij \rightarrow r$)	ECoN(ij)	PC(ij)		$V(r)$	MEFIR($ij \rightarrow r$)	$d(ij \rightarrow r)$	ECoN($ij \rightarrow r$)	ECoN(ij)
S	1	Se	0.138	2.256	1.00	4.00	Se	1	S	2.118	2.257	2.00	3.00
		O	0.131	1.446	3.00				K	1.909	3.756	1.00	
S	2	Se	0.138	2.257	1.00	4.00	O	1	S	1.320	1.451	1.00	3.87
		O	0.130	1.443	3.00				K	1.185	2.931	2.87	
K	1	Se	–	–	–	5.86	O	2	S	1.319	1.450	1.00	2.94
		O	1.634	2.743	5.86				K	1.157	2.853	1.94	
K	2	Se	1.847	3.756	1.00	8.30	O	3	S	1.309	1.439	1.00	3.00
		O	1.687	2.833	7.30				K	1.080	2.669	2.00	
							O	4	S	1.315	1.445	1.00	3.94
									K	1.160	2.867	2.94	
							O	5	S	1.317	1.448	1.00	4.00
									K	1.121	2.771	3.00	
							O	6	S	1.306	1.436	1.00	2.00
									K	1.076	2.655	1.00	

In the following we give a detailed description of the calculation procedure to illustrate step-by-step the new developments of the CHARDI method, in particular the iterative procedure to distribute the formal charge to each subpolyhedron.

Because the structure is based on heteroligand polyhedra in both the cation-centred and the anion-centred description, the first step consists of separating Q as a function of ECoN($ij \rightarrow r$)/ECoN(ij), equation (16′). This is first performed in the cation-centred description, but it could well be done on the anion-centred one. The result is then used to calculate $\Delta Q(i \rightarrow rs)$, equation (15), and $\Delta Q(ij \rightarrow r)$, equation (16), in an iterative cycle. Table 16 illustrates the procedure, which takes three steps to reach convergence on a threshold at 0.01 of ΔQ. In the first step, $\Delta Q(ij \rightarrow r)$ is obtained by separating $q(ij)$ as a function of ECoN($ij \rightarrow r$)/ECoN(ij), equation (16′). For both S atoms, ECoN(S $\rightarrow$ Se) = 1.00 and ECoN(S $\rightarrow$ O) = 3.00 so that $\frac{1}{4}$ of the formal charge (+6) is assumed to be distributed to Se and $\frac{3}{4}$ to O. K1 is not bound to Se and only distributes its formal charge to O atoms. Finally, ECoN(K $\rightarrow$ Se) = 1.00 and ECoN(S $\rightarrow$ O) = 7.31 so that 13.7% of the formal charge (+1) is assumed to be distributed to Se and 86.3% to O. This leads to a satisfactory charge distribution on the PC atoms (5.97 and 5.89 for S1 and S2, 1.10 and 1.03 for K1 and K2, respectively: MAPD 3.9%) but a largely unbalanced distribution on the V atoms, with Se severely overbonded (−3.12) and O atoms underbonded (−1.72 to −1.91) with MAPD = 16% (Table 17, 'step 1, cation-centred'). At this first step, the longer bonds are clearly overestimated but this is not an obstacle in the iterative procedure.

In the next step, the role of the PC and V atoms is exchanged. $\Delta q(ij \rightarrow rs)$ obtained from the cation-centred analysis are summed up around each chemical species of cation resulting in $\Delta Q(i \rightarrow rs)$ [equation (15)], then the roles of cations and anions are exchanged and $\Delta Q(ij \rightarrow r)$ which is to be used in the next step is computed through equation (16). This numerically corresponds to a simple change of sign, with the fundamental difference that the values are now collected about the anions. This corresponds to the exchange of indices $r \rightarrow i$, $s \rightarrow j$, $i \rightarrow r$, described in the previous section. For example, $\Delta Q(1 \rightarrow 25)$, which corresponds to ΔQ(K $\rightarrow$ O5), becomes ΔQ(O5 $\rightarrow$ K), which in the anion-centred description is $\Delta Q(25 \rightarrow 1)$. These values are used to compute the charge distribution whose results are in Table 17 ('step 1, anion-centred' in both tables). The procedure is then repeated by again swapping the roles of cations and anions until close values of $\Delta Q(ij \rightarrow r)$ are obtained between two cycles (convergence criterion used in this calculation: difference lower than 0.01 charge units: Δ columns in Table 16), which are obtained in three steps. The results in Table 17 are satisfactory in both descriptions and the differences between the second and the third step are minimal, as would be expected by the small differences (Δ) in Table 16 between these two steps.

5.5. Lanthanum orthosilicate selenide

We have previously used the structure of La_2SeSiO_4 (Brennan & Ibers, 1991) as an example of a compound containing heteroligand polyhedra treated with the scale factor algorithm (Nespolo *et al.*, 2001). In Tables 18 and 19 we present the results obtained with the new algorithm and reproduce the results published at that time, with the only difference being that the data dispersion is now presented in terms of MAPD. The results are practically unchanged; however, the new algorithm does not depend on any *a priori* assumption, as in the case of the previous one when an overall balance on the chemical species of the anions was assumed and used to compute the scale factors. The results obtained with the new algorithm are therefore unbiased.

Furthermore, we present the analysis of the anion-centred description (Tables 20 and 21), which were not accessible in the previous version. The results are also satisfactory in this description.

5.6. Disodium magnesium digadolinium *catena*-tetrasilicate difluoride

The structure of $Na_2MgGd_2(Si_4O_{12})F_2$ was reported by Maisonneuve & Leblanc (1998). We use this structure as a meaningful test because it contains various kinds of hetero-

electronic reprint

Table 16
Iterative calculation of $\Delta Q(ij \rightarrow r)$ of $K_2SeS_2O_6$.

Step 1

Cation-centred				Anion-centred						
PC(*ij*)	*V* (*r*)	$\Delta Q(ij \rightarrow r)$	Δ	PC(*i*)	*V* (*rs*)	$\Delta Q(i \rightarrow rs)$	PC(*ij*)	*V* (*r*)	$\Delta Q(ij \rightarrow r)$	Δ
S1	Se	1.501	–	S	Se	1.923	Se	S	−1.923	–
	O	4.499	–		O1	1.674		K	−0.077	–
S2	Se	1.500	–		O2	1.715	O1	S	−1.674	–
	O	4.500	–		O3	1.623		K	−0.326	–
K1	Se	0	–		O4	1.619	O2	S	−1.715	–
	O	1.000	–		O5	1.544		K	−0.285	–
K2	Se	0.120	–		O6	1.767	O3	S	−1.623	–
	O	0.880	–	K	Se	0.077		K	−0.377	–
					O1	0.326	O4	S	−1.619	–
					O2	0.285		K	−0.381	–
					O3	0.377	O5	S	−1.544	–
					O4	0.381		K	−0.456	–
					O5	0.456	O6	S	−1.767	–
					O6	0.233		K	−0.233	–

Step 2

Cation-centred							Anion-centred						
PC(*i*)	*V*(*rs*)	$\Delta Q(i \rightarrow rs)$	PC(*ij*)	*V*(*r*)	$\Delta Q(ij \rightarrow r)$	Δ	PC(*i*)	*V*(*rs*)	$\Delta Q(i \rightarrow rs)$	PC(*ij*)	*V*(*r*)	$\Delta Q(ij \rightarrow r)$	Δ
Se	S1	−0.966	S1	Se	0.966	0.534	S	Se	1.931	Se	S	−1.931	0.008
	S2	−0.978		O	5.034	0.534		O1	1.636		K	−0.069	0.008
	K1	0	S2	Se	0.978	0.522		O2	1.737	O1	S	−1.696	0.021
	K2	−0.069		O	5.022	0.522		O3	1.649		K	−0.304	0.021
O	S1	−5.034	K1	Se	0	0.000		O4	1.642	O2	S	−1.737	0.022
	S2	−5.022		O	1.000	0.000		O5	1.570		K	−0.263	0.022
	K1	−1.000	K2	Se	0.069	0.051		O6	1.789	O3	S	−1.649	0.026
	K2	−0.931		O	0.931	0.051	K	Se	0.069		K	−0.351	0.026
								O1	0.304	O4	S	−1.642	0.023
								O2	0.263		K	−0.358	0.023
								O3	0.351	O5	S	−1.570	0.026
								O4	0.358		K	−0.430	0.026
								O5	0.430	O6	S	−1.789	0.022
								O6	-0.211		K	−0.211	0.022

Step 3

Cation-centred							Anion-centred						
PC(*i*)	*V*(*rs*)	$\Delta Q(i \rightarrow rs)$	PC(*ij*)	*V*(*r*)	$\Delta Q(ij \rightarrow r)$	Δ	PC(*i*)	*V*(*rs*)	$\Delta Q(i \rightarrow rs)$	PC(*ij*)	*V*(*r*)	$\Delta Q(ij \rightarrow r)$	Δ
Se	S1	−0.959	S1	Se	0.959	0.008	S	Se	1.933	Se	S	−1.933	0.002
	S2	−0.970		O	5.041	0.008		O1	1.695		K	−0.067	0.002
	K1	0	S2	Se	0.970	0.008		O2	1.737	O1	S	−1.695	0.000
	K2	−0.066		O	5.030	0.008		O3	1.649		K	−0.305	0.000
O	S1	−5.041	K1	Se	0	0.000		O4	1.642	O2	S	−1.737	0.000
	S2	−5.030		O	1.000	0.000		O5	1.570		K	−0.263	0.000
	K1	−1.000	K2	Se	0.066	0.003		O6	1.789	O3	S	−1.649	0.000
	K2	−0.934		O	0.934	0.003	K	Se	0.067		K	−0.351	0.000
								O1	0.305	O4	S	−1.642	0.000
								O2	0.263		K	−0.358	0.000
								O3	0.351	O5	S	−1.570	0.000
								O4	0.358		K	−0.430	0.000
								O5	0.430	O6	S	−1.789	0.000
								O6	0.211		K	−0.211	0.000

ligand polyhedra, two in the cation-centred description (O and F), four in the anion-centred description (Na, Mg, Gd and Si), the latter including atoms of widely different size. The two Si atoms form somewhat distorted tetrahedra, Gd is coordinated by two F atoms and five O atoms (a sixth bond having a weight of 0.083 can be considered practically absent), Mg forms an hetero-octahedron with 2F and 6O, Na is coordinated by 1F and 6O (a seventh bond having a weight of 0.027 can be considered practically absent; Table 22). The results of the CHARDI analysis (Table 23) are quite satisfactory, with only a small OUB effect (O1 *versus* O3). In the anion-centred description (Tables 24 and 25) the result are even better.

electronic reprint

Table 17
Computed charges of $K_2SeS_2O_6$ as a function of $\Delta Q(ij \rightarrow r)$ obtained by the iterative procedure in Table 16.

Step 1												Step 2												Step 3											
Cation-centred						Anion-centred						Cation-centred						Anion-centred						Cation-centred								Anion-centred			
PC(ij)		Q	$V(rs)$		Q	PC(ij)		Q	$V(rs)$		Q	PC(ij)		Q	$V(rs)$		Q	PC(ij)		Q	$V(rs)$		Q	PC(ij)		Q	r	s	Q	PC(ij)		$QV(rs)$	$V(rs)$		Q
S	1	5.97	Se	1	−3.12	Se	1	−2.01	S	1	5.97	S	1	6.04	Se	1	−2.01	Se	1	−2.00	S	1	6.05	S	1	6.04	Se	1	−2.01	Se	1	−2.00	S	1	6.04
S	2	5.89	O	1	−1.76	O	1	−1.98	S	2	5.89	S	2	5.97	O	1	−1.94	O	1	−1.99	S	2	5.97	S	2	5.97	O	1	−1.95	O	1	−1.99	S	2	5.97
K	1	1.10	O	2	−1.72	O	2	−1.99	K	1	1.02	K	1	1.00	O	2	−1.91	O	2	−1.99	K	1	0.95	K	1	1.00	O	2	−1.91	O	2	−1.99	K	1	0.95
K	2	1.03	O	3	−1.91	O	3	−1.98	K	2	1.11	K	2	0.99	O	3	−2.10	O	3	−1.99	K	2	1.04	K	2	0.99	O	3	−2.10	O	3	−1.99	K	2	1.03
			O	4	−1.83	O	4	−2.00							O	4	−2.02	O	4	−2.01							O	4	−2.02	O	4	−2.01			
			O	5	−1.91	O	5	−2.00							O	5	−2.09	O	5	−2.01							O	5	−2.10	O	5	−2.01			
			O	6	−1.75	O	6	−2.03							O	6	−1.93	O	6	−2.02							O	6	−1.93	O	6	−2.02			
MAPD		3.9			16.0			0.6			3.9			0.7			3.2			0.5			2.5		0.7			3.2			0.5			2.4

Table 18
Bond distances d (Å), FIR (Å) and bond weights of La_2SeSiO_4 (Brennan & Ibers, 1991) in the cation-centred description.

The structure is built by heteroligand polyhedra.

PC(ij)		$q(ij)$	$h(ij)$	$V(rs)$		$q(rs)$	$h(rs)$	$d(ij \rightarrow rs)$	FIR($ij \rightarrow rs$)	
La	1	3.00	4	O	1	−2.00	8	2.5007 × 2	1.229 × 2	1.081 × 2
				O	1	−2.00	8	2.5169 × 2	1.237 × 2	1.043 × 2
				O	2	−2.00	8	2.6014 × 2	1.279 × 2	0.845 × 2
				Se	1	−2.00	4	3.0476	1.185	1.267
				Se	1	−2.00	4	3.2324	1.256	0.917
				Se	1	−2.00	4	3.5407	1.376	0.416
La	2	3.00	4	O	2	−2.00	8	2.5096 × 2	1.234 × 2	1.052 × 2
				O	1	−2.00	8	2.5315 × 2	1.244 × 2	1.000 × 2
				O	2	−2.00	8	2.5561 × 2	1.257 × 2	0.942 × 2
				Se	1	−2.00	4	3.2329 × 2	1.257 × 2	1.210 × 2
				Se	1	−2.00	4	3.7827 × 2	1.470 × 2	0.341 × 2
Si	1	4.00	4	O	2	−2.00	8	1.6302 × 2	0.405 × 2	1.017 × 2
				O	1	−2.00	8	1.6395 × 2	0.407 × 2	0.983 × 2

5.7. $KMoO_2PO_4$: a non-Madelung-type structure on which CHARDI cannot work

Molybdates in which bonds of different order coexist in the same polyhedron can be represented by the title compound (Peascoe & Clearfield, 1991). Here the coordination of molybdenum is of type 2 + 4 with a large gap between the two shortest bond distances and the four longer ones (Tables 26 and 28). With respect to the crocoite example analysed above, no resonance appears to occur, as shown by the largely different bond distances. Adoption of the iterative calculation of the bond weights (Nespolo *et al.*, 2001) is normally capable of correctly treating distorted polyhedra. In this case, however, the gap is too wide and the bond weights attributed to the longer distances are too small to obtain the input charge $q(ij)$ as a result of the distribution procedure. Indeed, the results on both descriptions, cation-centred (Table 27) and anion-centred (Table 29), are unsatisfactory. This type of structure is not correctly described in a Madelung-type framework and remains outside the possibilities of a satisfactory CHARDI analysis.

6. Discussion

The concept of bond strength has its roots in the XIX century theory of valence and is based on the idea that the total bond valence received by each atom is equal to its atomic valence. The CHARDI method fundamentally differs from other methods that investigate the connectivity of a crystal structure in term of the network of bond strengths in being essentially a geometric analysis of the coordination polyhedra exploiting the observed distances only, rather than comparing them with some 'standard values' which actually undergo frequent redefinition and re-refinement. The bond weight is a purely geometric concept which quantitatively tells how strongly the presence of a V atom at the corner of a polyhedron is felt by the PC atom at the centre of it. The bond weight is not directly related to the electron density of the bond and the charge is distributed, and not computed, among each bond and the equivalent of the valence sum rule (or bond valence sum, BVS) strictly applies to $Q(ij)$, not to $Q(rs)$, the two quantities bringing different information: a measure of the OUB effects

Table 19
MEFIR (Å), ECoN and computed charges of La_2SeSiO_4 in the cation-centred description.

CHARDI (2015)												CHARDI (2001)						CHARDI (1999)					
PC(ij)		$V(r)$	MEFIR($ij \rightarrow r$)	$d(ij \rightarrow r)$	ECoN($ij \rightarrow r$)	ECoN(ij)	Q	$V(rs)$		Q		PC(ij)	Q	$V(rs)$		Q		PC(ij)	Q	$V(rs)$		Q	
La	1	O	1.246	2.535	5.94	8.54	2.99	O	1	−2.02		La 1	2.99	O	1	−2.00		La 1	3.00	O	1	−1.89	
		Se	1.239	3.188	2.60																		
La	2	O	1.244	2.532	5.99	9.09	3.01	O	2	−1.98		La 2	3.01	O	2	−2.03		La 2	3.05	O	2	−2.07	
		Se	1.301	3.349	3.10																		
Si	1	O	1.635	1.635	4.00	4.00	4.00	Se	1	−2.00		Si 1	4.00	Se	1	−1.97		Si 1	3.95	Se	1	-1.98_5	
		Se																					
MAPD							0.2			0.9			0.2			0.9			1.0			3.8	

electronic reprint

Table 20
Bond distances d (Å), FIR (Å) and bond weights of La_2SeSiO_4 in the anion-centred description.

The structure is built by heteroligand polyhedra.

PC(ij)		$q(ij)$	$h(ij)$	$V(rs)$		$q(rs)$	$h(rs)$	$d(ij \rightarrow rs)$	FIR($ij \rightarrow rs$)	
O	1	−2	8	La	1	3	4	2.5007	1.271	1.037
				La	1	3	4	2.5169	1.280	0.998
				La	2	3	4	2.5315	1.287	0.963
				Si	1	4	4	1.6395	1.232	1.000
O	2	−2	8	La	2	3	4	2.5096	1.276	1.101
				La	2	3	4	2.5561	1.300	0.991
				La	1	3	4	2.6014	1.323	0.886
				Si	1	4	4	1.6302	1.225	1.000
Se	1	−2	4	La	1	3	4	3.0476	1.863	1.388
				La	1	3	4	3.2324	1.976	1.044
				La	2	3	4	3.2329 × 2	1.976 × 2	1.043 × 2
				La	1	3	4	3.5407	2.164	0.521
				La	2	3	4	3.7827 × 2	2.312 × 2	0.233 × 2

Table 21
MEFIR (Å), ECoN and computed charges of La_2SeSiO_4 in the anion-centred description.

PC(ij)		$V(r)$	MEFIR ($ij \rightarrow r$)	$d(ij \rightarrow r)$	ECoN ($ij \rightarrow r$)	ECoN(ij)	Q	$V(rs)$		Q
O	1	La	1.279	2.516	3.00	4.00	−1.99	La	1	3.05
		Si	1.232	1.639	1.00					
O	2	La	1.298	2.552	2.98	3.98	−2.01	La	2	2.95
		Si	1.225	1.630	1.00					
Se	1	La	1.990	3.256	5.50	5.50	−2.00	Si	1	4.00
		Si	–	–	–		–			
MAPD							0.3			1.0

Table 22
Bond distances d (Å), FIR (Å) and bond weights of $Na_2MgGd_2(Si_4O_{12})F_2$ (Maisonneuve & Leblanc, 1998) in the cation-centred description.

The structure is built by heteroligand polyhedra.

PC(ij)		$q(ij)$	$h(ij)$	$V(rs)$		$q(rs)$	$h(rs)$	$d(ij \rightarrow rs)$	FIR($ij \rightarrow rs$)	
Gd	1	3	4	F	1	−1	4	2.4712	1.197	1.003
				F	1	−1	4	2.4735	1.198	0.997
				O	5	−2	4	2.2750	1.073	1.136
				O	6	−2	4	2.2878	1.079	1.103
				O	2	−2	4	2.3167	1.093	1.027
				O	4	−2	4	2.3490	1.108	0.944
				O	6	−2	4	2.3921	1.128	0.836
				O	3	−2	4	2.8666	1.352	0.083
Si	1	4	4	O	2	−2	4	1.5943	0.396	1.115
				O	4	−2	4	1.6021	0.398	1.086
				O	1	−2	4	1.6444	0.409	0.930
				O	3	−2	4	1.6780	0.417	0.809
Si	2	4	4	O	5	−2	4	1.6107	0.400	1.079
				O	6	−2	4	1.6137	0.401	1.068
				O	1	−2	4	1.6494	0.410	0.937
				O	3	−2	4	1.6622	0.413	0.890
Mg	1	2	2	F	1	−1	4	1.9704	0.843	1.000
				F	1	−1	4	1.9704	0.843	1.000
				O	4	−2	4	2.0868 × 2	0.867 × 2	1.003 × 2
				O	5	−2	4	2.0889 × 2	0.868 × 2	0.997 × 2
Na	1	1	4	F	1	−1	4	2.3165	1.322	1.000
				O	2	−2	4	2.3711	1.324	1.397
				O	1	−2	4	2.5381	1.417	0.998
				O	4	−2	4	2.5509 × 2	1.424 × 2	0.968 × 2
				O	3	−2	4	2.7302	1.525	0.576
				O	1	−2	4	2.9554	1.650	0.224
				O	5	−2	4	3.2745	1.828	0.027

Table 23
MEFIR (Å), ECoN and computed charges of $Na_2MgGd_2(Si_4O_{12})F_2$ in the cation-centred description.

PC(ij)		$V(r)$	MEFIR ($ij \rightarrow r$)	$d(ij \rightarrow r)$	ECoN ($ij \rightarrow r$)	ECoN(ij)	Q	$V(rs)$		Q
Gd	1	F	1.197	2.472	2.00	7.13	3.00	F	1	−1.01
	1	O	1.097	2.327	5.13			O1	1	−2.09
Si	1	F	–	–	–	3.94	3.98	O2	2	−2.01
		O	0.404	1.625	3.94			O3	3	−1.85
Si	2	F	–	–	–	3.97	4.05	O4	4	−2.08
		O	0.405	1.632	3.97			O5	5	−1.99
Mg	1	F	0.843	1.970	2.00	6.00	1.98	O6	6	−1.97
	1	O	0.867	2.088	4.00					
Na	1	F	1.322	2.317	1.00	6.15	0.99			
	1	O	1.416	2.537	5.15					
MAPD							0.8			2.7

for $Q(rs)$, the evaluation of the applicability – including structure reliability – for $Q(ij)$.

One aspect that the CHARDI method originally inherited from the old valence theory assumed the cations to be the centre of the coordination polyhedra. This limitation has been recently removed (Eon & Nespolo, 2015) and the new route to treat heteroligand polyhedra presented here allows CHARDI to be free from the few assumptions it still had in the previous versions. The need for a scaling factor in the treatment of heteroligand polyhedra, which were computed under the assumption of an overall charge balance on the same chemical species of anions, has been removed. Furthermore, the empirical estimation of the minimal PC—V distance corresponding to a bonding contact has been effectively replaced by the use of MEFIR in the first step of the analysis of the coordination polyhedra.

Despite the Madelung-type approach, CHARDI has proved to be able to treat a wide range of structures with a large chemical heterogeneity, although some types of compounds still remain outside its possibilities, as shown by the example of $KMoO_2PO_4$ discussed above. Apart from these rare exceptions, CHARDI can bring important information not always easily obtained from experimental data:

(i) a structure validation based only on internal criteria, without the reference to empirical parameters (see *e.g.* Tmar Trabelsi *et al.*, 2015);

(ii) the presence of structural anomalies, as in the case of pyroxenes analysed by Nespolo *et al.* (1999);

(iii) the site-occupancy factor of incompletely occupied sites (see *e.g.* Guesmi *et al.*, 2006);

(iv) the most likely oxidation state of atoms with multiple valences (see *e.g.* Pignatelli *et al.*, 2011);

(v) the most likely oxidation state of an atomic site in compounds presenting isomorphic substitutions, which gives a clear indication of the fractional occupancy by each type of atom (see *e.g.* Toumi & Mhiri, 2008): this information may be difficult to obtain from conventional X-ray diffraction experiments in the case of heterovalent substitutions involving

electronic reprint

Table 24
Bond distances d (Å), FIR (Å) and bond weights of $Na_2MgGd_2(Si_4O_{12})F_2$ in the anion-centred description.

The structure is built by heteroligand polyhedra.

PC(ij)		$q(ij)$	$h(ij)$	$V(rs)$		$q(rs)$	$h(rs)$	$d(ij \rightarrow rs)$	FIR($ij \rightarrow rs$)	
F	1	−1	4	Gd	1	3	4	2.4712	1.274	1.003
				Gd	1	3	4	2.4735	1.276	0.997
				Mg	1	2	2	1.9704	1.127	1.000
				Na	1	1	4	2.3165	0.994	1.000
O	1	−2	4	Si	1	4	4	1.6444	1.236	1.009
				Si	2	4	4	1.6494	1.240	0.991
				Na	1	1	4	2.5381	1.121	1.213
				Na	1	1	4	2.9554	1.305	0.364
O	2	−2	4	Gd	1	3	4	2.3167	1.224	1.000
				Si	1	4	4	1.5943	1.198	1.000
				Na	1	1	4	2.3711	1.047	1.17
				Na	1	1	4	2.5509	1.126	0.735
O	3	−2	4	Gd	1	3	4	2.8666	1.515	1.000
				Si	2	4	4	1.6622	1.249	1.028
				Si	1	4	4	1.6780	1.261	0.971
				Na	1	1	4	2.7302	1.206	1.000
O	4	−2	4	Gd	1	3	4	2.3490	1.241	1.000
				Si	1	4	4	1.6021	1.204	1.000
				Mg	1	2	2	2.0868	1.220	1.000
				Na	1	1	4	2.5509	1.126	1.000
O	5	−2	4	Gd	1	3	4	2.2750	1.202	1.000
				Si	2	4	4	1.6107	1.211	1.000
				Mg	1	2	2	2.0889	1.221	1.000
				Na	1	1	4	3.2745	1.446	1.000
O	6	−2	4	Gd	1	3	4	2.2878	1.209	1.116
				Gd	1	3	4	2.3921	1.264	0.849
				Si	2	4	4	1.6137	1.213	1.000
				Na	1	1	4	3.5549	1.570	1.000

Table 25
MEFIR (Å), ECoN and computed charges of $Na_2MgGd_2(Si_4O_{12})F_2$ in the anion-centred description.

PC(ij)		$V(r)$	MEFIR ($ij \rightarrow r$)	$d(ij \rightarrow r)$	ECoN ($ij \rightarrow r$)	ECoN(ij)	Q	$V(rs)$		Q
F	1	Gd	1.275	2.472	2	4.00	−1.01	Gd	1	3.00
F	1	Si	–	–	–			Si	1	4.00
F	1	Mg	1.127	1.97	1			Si	2	4.03
F	1	Na	0.994	2.317	1			Mg	1	1.97
O	1	Si	1.238	1.647	2	3.58	−2.00	Na	1	0.99
O	1	Mg	–	–	–					
O	1	Na	1.161	2.631	1.58					
O	2	Gd	1.224	2.317	1					
O	2	Si	1.198	1.594	1	3.90	−2.01			
O	2	Mg	–	–	–					
O	2	Na	1.077	2.439	1.9					
O	3	Gd	1.521	2.867	1					
O	3	Si	1.255	1.67	2	4.00	−1.99			
O	3	Na	1.206	2.73	1					
O	4	Gd	1.241	2.349	1					
O	4	Si	1.204	1.602	1					
O	4	Mg	1.220	2.087	1	4.00	−2.01			
O	4	Na	1.126	2.551	1					
O	5	Gd	1.202	2.275	1					
O	5	Si	1.211	1.611	1					
O	5	Mg	1.221	2.089	1	4.00	−2.00			
O	5	Na	1.446	3.275	1					
O	6	Gd	1.232	2.332	1.96					
O	6	Si	1.213	1.614	1					
O	6	Mg	–	–	–	3.96	–1.99			
O	6	Na	1.620	3.555	1					
F	1	Gd	1.275	2.472	2					
F	1	Si	–	–	–					
MAPD							0.3			0.6

Table 26
Bond distances d (Å), FIR (Å) and bond weights of $KMoO_2PO_4$ in the cation-centred description, where the structure is built by homoligand polyhedra.

PC(ij)		$q(ij)$	$h(ij)$	$V(rs)$		$q(rs)$	$h(rs)$	$d(ij \rightarrow rs)$	FIR($ij \rightarrow rs$)	$w(ij \rightarrow rs)$
Mo	1	6	16	O	3	−2	32	1.6919 × 2	0.529 × 2	1.278 × 2
				O	2	−2	32	1.9788 × 2	0.618 × 2	0.394 × 2
				O	1	−2	32	2.1907 × 2	0.685 × 2	0.078 × 2
K	1	1	16	O	3	−2	32	2.8062 × 2	1.671 × 2	1.294 × 2
				O	2	−2	32	2.8508 × 2	1.697 × 2	1.202 × 2
				O	1	−2	32	2.9521 × 2	1.757 × 2	0.994 × 2
				O	3	−2	32	3.2259 × 2	1.920 × 2	0.490 × 2
				O	1	−2	32	3.2984 × 2	1.964 × 2	0.384 × 2
P	1	5	16	O	1	−2	32	1.5112 × 2	0.308 × 2	1.091 × 2
				O	2	−2	32	1.5632 × 2	0.319 × 2	0.889 × 2

Table 27
MEFIR (Å), average distance d (Å), ECoN and computed charges of $KMoO_2PO_4$ in the cation-centred description.

PC(ij)		MEFIR(ij)	$d(ij)$	ECoN(ij)	Q	V (rs)		Q	$\Delta Q(i \rightarrow rs)$	
Mo	1	0.553	1.773	3.50	5.37	O	1	−1.67	O1—Mo	−0.160
K	1	1.754	2.949	8.72	1.00	O	2	−1.94	O1—K	−0.189
P	1	0.313	1.534	3.96	5.62	O	3	−2.40	O1—P	−1.651
									O2—Mo	−0.698
									O2—K	−0.142
									O2—P	−1.160
									O3—Mo	−1.829
									O3—K	−0.171
									O3—P	–
MAPD					7.8			13.2		

Table 28
Bond distances d (Å), FIR (Å) and bond weights of $KMoO_2PO_4$ (Peascoe & Clearfield, 1991) in the anion-centred description, where the structure is built by heteroligand polyhedra.

PC(ij)		$q(ij)$	$h(ij)$	$V(rs)$		$q(rs)$	$h(rs)$	$d(ij \rightarrow rs)$	FIR($ij \rightarrow rs$)	$w(ij \rightarrow rs)$
O	1	−2	32	Mo	1	6	16	2.1907	1.506	1.000
				K	1	1	16	2.9521	1.195	1.213
				K	1	1	16	3.2984	1.335	0.566
				P	1	5	16	1.5112	1.203	1.000
O	2	−2	32	Mo	1	6	16	1.9788	1.360	1.000
				K	1	1	16	2.8508	1.154	1.000
				P	1	5	16	1.5632	1.244	1.000
O	3	−2	32	Mo	1	6	16	1.6919	1.163	1.000
				K	1	1	16	2.8062	1.136	1.220
				K	1	1	16	3.2259	1.305	0.428

atoms of close atomic number or atoms with different valence states;

(vi) the most likely positions of missing light atoms (like hydrogen), who are hidden by the presence of relatively heavy atoms.

The extension and generalization presented in this work should allow an even wider application of the CHARDI approach and a complete exploitation of its full potential.

Acknowledgements

This research has been conducted during a stay as an invited professor at Kyoto University. We thank Dr Abderrahmen

electronic reprint

Table 29
MEFIR (Å), average distance d (Å), ECoN and computed charges of $KMoO_2PO_4$ in the anion-centred description.

PC(ij)		$V(r)$	MEFIR ($ij \rightarrow r$)	$d(ij \rightarrow r)$	ECoN ($ij \rightarrow r$)	ECoN(ij)	Q	V (rs)		Q
O	1	Mo	1.506	2.191	1.00	3.78	−1.84	Mo	1	5.37
		K	1.237	3.060	1.78		−1.95	K	1	1.00
		P	1.203	1.511	1.00		−2.21	P	1	5.62
O	2	Mo	1.360	1.979	1.00	3.00				
		K	1.161	2.851	1.00					
		P	1.244	1.563	1.00					
O	3	Mo	1.163	1.692	1.00	2.65				
		K	1.179	2.912	1.65					
		P	–	–	–					
MAPD							7.1			7.8

Guesmi (Université de Tunis El Manar, Tunisia) for pointing out the case of $KMoO_2PO_4$. Critical remarks by two anonymous reviewers are thankfully acknowledged.

References

Beck, H. P. (2014). *Z. Kristallogr.* **229**, 473–488.
Bosi, F. (2014*a*). *Acta Cryst.* B**70**, 697–704.
Bosi, F. (2014*b*). *Acta Cryst.* B**70**, 864–870.
Brennan, T. D. & Ibers, J. A. (1991). *Acta Cryst.* C**47**, 1062–1064.
Brown, I. D. (1977). *Acta Cryst.* B**33**, 1305–1310.
Brown, I. D. (1978). *Chem. Soc. Rev.* **7**, 359–376.
Effenberger, H. & Pertlik, F. (1986). *Z. Kristallogr.* **176**, 75–83.
Eon, J.-G. & Nespolo, M. (2015). *Acta Cryst.* B**71**, 34–47.
Foust, A. S. & Janickis, V. (1980). *Inorg. Chem.* **19**, 1063–1064.
Gagné, O. C. & Hawthorne, F. C. (2015). *Acta Cryst.* B**71**, 562–578.
Guesmi, A., Nespolo, M. & Driss, A. (2006). *J. Solid State Chem.* **179**, 2466–2471.
Hoppe, R. (1970). *Angew. Chem. Int. Ed. Engl.* **9**, 25–34.
Hoppe, R. (1979). *Z. Kristallogr.* **150**, 23–52.
Hoppe, R., Voigt, S., Glaum, H., Kissel, J., Müller, H. P. & Bernet, K. (1989). *J. Less-Common Met.* **156**, 105–122.
IUPAC (1997). *Compendium of Chemical Terminology*, 2nd ed. Compiled by A. D. McNaught & A. Wilkinson. Oxford: Blackwell Scientific Publications.
Maisonneuve, V. & Leblanc, M. (1998). *Can. Mineral.* **36**, 1039–1043.
Marquardt, M. A., Ashmore, N. A. & Cann, D. P. (2006). *Thin Solid Films*, **496**, 146–156.
Merlino, S., Pasero, M., Perchiazzi, N. & Kampf, A. R. (1996). *Am. Mineral.* **81**, 1277–1281.
Mohri, F. (2000). *Acta Cryst.* B**56**, 626–638.
Momma, K. & Izumi, F. (2011). *J. Appl. Cryst.* **44**, 1272–1276.
Nespolo, M., Ferraris, G., Ivaldi, G. & Hoppe, R. (2001). *Acta Cryst.* B**57**, 652–664.
Nespolo, M., Ferraris, G. & Ohashi, H. (1999). *Acta Cryst.* B**55**, 902–916.
Pauling, L. (1929). *J. Am. Chem. Soc.* **51**, 1010–1026.
Pauling, L. (1960). *The Nature of the Chemical Bond*, 3rd ed. Oxford University Press.
Peascoe, R. & Clearfield, A. (1991). *J. Solid State Chem.* **95**, 83–93.
Pendás, A. M., Costales, A. & Luaña, V. (1998). *J. Phys. Chem. B*, **102**, 6937–6948.
Pignatelli, I., Dusek, M., De Titta, G. & Nespolo, M. (2011). *Eur. J. Mineral.* **23**, 73–84.
Tmar Trabelsi, I., Oueslati, A., Mhiri, T. & Toumi, M. (2015). *J. Alloys Compd.* **641**, 14–21.
Toumi, M. & Mhiri, T. (2008). *Mater. Res. Bull.* **43**, 1346–1354.
Van Tendeloo, G., Garlea, O., Darie, C., Bougerol-Chaillout, C. & Bordet, P. (2001). *J. Solid State Chem.* **156**, 428–436.

electronic reprint